

Multi-agent Communication with Graph Information Bottleneck under Limited Bandwidth

Qi Tian¹, Kun Kuang¹, Baoxiang Wang^{2,3}, Furui Liu⁴, Fei Wu¹

¹College of Computer Science, Zhejiang University

²The Chinese University of Hong Kong, Shenzhen

³Shenzhen Institute of Artificial Intelligence and Robotics for Society

⁴Huawei Noah's Ark Lab

ABSTRACT

Recent studies have shown that introducing communication between agents can significantly improve overall performance in cooperative Multi-agent reinforcement learning (MARL). In many real-world scenarios, communication can be expensive and the bandwidth of the multi-agent system is subject to certain constraints. Redundant messages who occupy the communication resources can block the transmission of informative messages and thus jeopardize the performance. In this paper, we aim to learn the minimal sufficient communication messages. First, we initiate the communication between agents by a complete graph. Then we introduce the graph information bottleneck (GIB) principle into this complete graph and derive the optimization over graph structures. Based on the optimization, a novel multi-agent communication module, called CommGIB, is proposed, which effectively compresses the structure information and node information in the communication graph to deal with bandwidth-constrained settings. Extensive experiments in Traffic Control and StanCraft II are conducted. The results indicate that the proposed methods can achieve better performance in bandwidth-restricted settings compared with state-of-the-art algorithms, with especially large margins in large-scale multi-agent tasks.

CCS CONCEPTS

• **Theory of computation** → **Multi-agent reinforcement learning**; • **Mathematics of computing** → **Information theory**.

KEYWORDS

multi-agent reinforcement learning, bandwidth-constrained communication, information theory

ACM Reference Format:

Qi Tian¹, Kun Kuang¹, Baoxiang Wang^{2,3}, Furui Liu⁴, Fei Wu¹. 2018. Multi-agent Communication with Graph Information Bottleneck under Limited Bandwidth. In *Woodstock '18: ACM Symposium on Neural Gaze Detection, June 03–05, 2018, Woodstock, NY*. ACM, New York, NY, USA, 13 pages. <https://doi.org/10.1145/1122445.1122456>

Permission to make digital or hard copies of all or part of this work for personal or classroom use is granted without fee provided that copies are not made or distributed for profit or commercial advantage and that copies bear this notice and the full citation on the first page. Copyrights for components of this work owned by others than ACM must be honored. Abstracting with credit is permitted. To copy otherwise, or republish, to post on servers or to redistribute to lists, requires prior specific permission and/or a fee. Request permissions from permissions@acm.org.

Woodstock '18, June 03–05, 2018, Woodstock, NY

© 2018 Association for Computing Machinery.

ACM ISBN 978-1-4503-XXXX-X/18/06...\$15.00

<https://doi.org/10.1145/1122445.1122456>

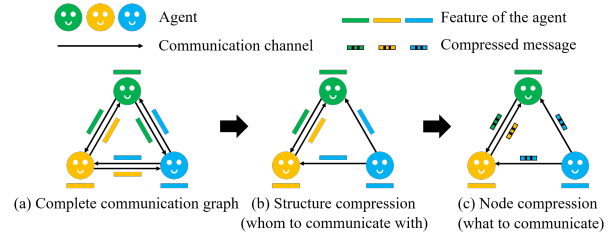


Figure 1: An illustration of graph structure and node information compression in CGIBNet. (a) A directed complete graph is proposed to model multi-agent communication. (b) Graph structure compression is design for identifying whom to communicate with. (c) Node information compression is used to learn what to communicate.

1 INTRODUCTION

Multi-agent reinforcement learning has shown its powerful ability to cope with many challenging problems, including autonomous driving [24], game playing [25] and swarm robotics [8]. In these scenarios, the communication mechanism is regarded as a promising way to propagate the beliefs of the agents, leading to a better groups' coordination. Thus, a variety of works have been proposed in the field of multi-agent communication to improve the performance of MARL [1, 3, 5, 6, 11, 12, 14, 18, 20, 22, 28].

In real multi-agent systems, however, communication resources are usually limited. Under this setting, the key problem is how to efficiently exploit the available bandwidth and reduce the redundant communication among multi-agents. Hence, we face the following challenges for bandwidth-constrained communication in MARL: (1) **Who to communicate with?** Each agent needs to identify the agents that are necessary to communicate with for a good performance and establish an efficient cooperation protocol among multiple agents. (2) **What to communicate?** Each agent needs to deliver a concise and compact message, otherwise one large message may occupy the whole communication resources.

Recently, many methods [13, 16, 27, 31, 32] have been proposed to address the above challenges, but they have the following shortcomings: 1) Existing methods only focus on one of the challenges, not both. *e.g.*, [13, 16, 27] solve the first challenge, while [31, 32] solve the second. An intuitive idea is to combine these methods to simultaneously overcome the above challenges. However, due to the lack of unified theoretical guidance and some compatibility

problems, this combination can only achieve sub-optimal performance. 2) Many previous methods [13, 27, 31] need to learn an extra actor for message aggregation, hence are limited to policy-based MARL frameworks and cannot be applied into value-based MARL frameworks [4]. 3) All methods are designed for single-round communication and cannot compress the communication bandwidth in multiple rounds of communication.

Based on the above discussion, in this paper, we focus on the problem of bandwidth-constrained communication in MARL. To simultaneously address the challenges of whom to communicate with and what to communicate, we propose a novel and universal multi-agent communication model named Communicative Graph Information Bottleneck Network (CGIBNet). Specifically, we first model multi-agent communication with a directed complete graph as is shown in Figure 1(a). Then we derive two optimizable variational upper bounds based on the graph information bottleneck (GIB) principle and instantiate them into two regularizers to compress graph structure and node information. The first regularizer is designed for addressing the challenge of whom to communicate with as is shown in Figure 1(b), by reducing the unnecessary communication channels between agents and maximally preserving information for decision-making. Moreover, in the setting of multi-round communication, this regularizer can also be used in each layer of the graph to reduce communication overhead in each communication round. The second regularizer is designed for solving the problem of what to communicate as is shown in Figure 1(c), by learning compact node representations to reduce bandwidth occupancy. Since the structure learning of CGIBNet is modeled as a link prediction task [34] instead of an actor-based scheduler, our model is learned implicitly with downstream reinforcement learning tasks in an end-to-end manner and can be easily applied to the existing MARL frameworks (*i.e.*, policy-based and value-based MARL). We summarize our contributions as follows:

- We investigate the problem of bandwidth-constrained communication in MARL by simultaneously considering with whom and what to communicate, and give theoretical analysis and optimization surrogate to address this problem through the GIB principle.
- We propose our novel CGIBNet based on the GIB principle, to jointly compress the structure and node information of communication graph for identification of with whom and what to communicate. CGIBNet is a universal module, which can be easily plugged into both policy-based and value-based MARL.
- Experiments on both Traffic Control and StarCraftII show that our proposed method outperforms the state-of-the-art algorithms (including their combination), and the margins are especially large for large-scale multi-agent systems.

2 RELATED WORK

MARL communication. A variety of works have been proposed to explore communication protocols in MARL, including message aggregation [3, 11, 28], memory-driven communication [20], *etc.* To efficiently utilize finite communication resources, some recent MARL methods introduce various gating mechanisms to reduce communication channels between agents. *e.g.*, IC3Net [27] models

the gate by learning an extra actor, while G2A [16] achieves this goal through hard attention and combines with soft attention to improving its performance. However, these methods still need frequent communication. SchedNet [13] leverages a weight generator to explicitly restrict bandwidth occupancy, but this method requires each agent to always communicate with a predefined number of other agents even if the agent can make the optimal decision based on its own private observation. Also, This method is not suitable for value-based MARL since the generator is modeled as an actor. Another direction is to compress node message representations to save communication resources. *e.g.*, NDQ [32] and IMAC [31] introduce a specific regularizer based on information theory to achieve this goal, but these methods rely on fully connected communication, resulting in sub-optimal message representations and poor performance in some specific scenarios. *e.g.*, target communication is needed [3]. In this paper, we simultaneously schedule communication channels and compress node representations under a unified framework through the graph information bottleneck principle and overcome all their shortcomings.

Information bottleneck. Information bottleneck (IB), originally proposed for signal processing, tries to find a short code of the input signal but preserves maximum information of the code [30]. Alemi et al. [2] first introduces the IB into deep neural networks, then the IB is applied to various domains [9, 19, 21]. Recently, Wu et al. [33] extend the IB theory to the graph data to learn compact node representations, which can improve model robustness against adversarial examples. However, they assume that the graph data satisfies the local-dependence assumption and the underlying graph is a static graph, while we deal with a dynamic graph (*i.e.*, communication graph), leading to differences between our method and their method in terms of both theoretical derivation and instantiation.

3 PRELIMINARY

In this section, we first present the problem setting of MARL communication. Then, we give a brief introduction of policy-based and value-based MARL with communication since we apply these frameworks for evaluation.

DEC-POMDP with Communication. MARL communication is extended from Decentralized Partially Observable Markov Decision Process (Dec-POMDP) and defined as a tuple $\langle N, \mathcal{S}, \mathcal{A}, \mathcal{T}, \mathcal{R}, \mathcal{O}, \mathcal{M}, \Omega, \gamma \rangle$, where N represents the number of agents; \mathcal{S} represents the state space of the environment; $\mathcal{A} = \{\mathcal{A}_i\}_{i=1,2,\dots,N}$ represents the set of actions; $\mathcal{T}(s'|s, \mathbf{a}) : \mathcal{S} \times \mathcal{A} \rightarrow \mathcal{S}$ represents the state transition function and $\mathbf{a} = [a_1, a_2, \dots, a_N]$ denotes the joint action space; $\mathcal{R} = \{\mathcal{R}_i\}_{i=1,2,\dots,N} : \mathcal{S} \times \mathcal{A} \rightarrow \mathbb{R}^N$ represents the set of reward functions, and it can be one shared reward in some settings; $\mathcal{O} = \{\mathcal{O}_i\}_{i=1,2,\dots,N}$ represents the set of local observations for all agents; $\Omega(s, i) : \mathcal{S} \rightarrow \mathcal{O}_i$ is the observation function that determines the local observation of agent i ; γ represents the discount factor; $\mathcal{M} = \{m_i\}_{i=1,2,\dots,N}$ represents the space of messages, where m_i denotes the message sent by agent i and it is usually obtained by encoding the local observation $m_i = \Psi(o_i)$. Each agent will receive messages $\mathbf{m}_{-i} = [m_1, \dots, m_{i-1}, m_{i+1}, \dots, m_N]$ sent by its cooperators to make better decisions.

Policy-based MARL with communication. MAPPO [?] is one of the most successful works in policy-based MARL, and we modify it for MARL communication evaluation. Specifically, the parameter θ_i of each agent π_{θ_i} is updated based on the policy gradient theorem [29] with clipping probability ratio ρ_{θ_i} , thus the gradient of the objective is

$$\nabla_{\theta_i} \mathcal{L}_{MARL,i}^{MAPPO} = \mathbb{E}_{s, a_i \sim \tau} [\min(\rho_{\theta_i} A(s, \mathbf{a}), \text{clip}(\rho_{\theta_i}, 1-\epsilon, 1+\epsilon) A(s, \mathbf{a}))], \quad (1)$$

where τ is the trajectory distribution, ϵ is a hyperparameter to control the feasible range of policy update, ρ_{θ_i} is the probability ratio of the current policy π_{θ_i} to the old policy $\pi_{\theta_i, old}$, i.e., $\pi_{\theta_i}(a_i|o_i, \mathbf{m}_{-i}) / \pi_{\theta_i, old}(a_i|o_i, \mathbf{m}_{-i})$. $A(s, \mathbf{a})$ is the advantage function defined as $\sum_{k=t}^T \gamma^{k-t} R_t - V_{\phi}(s, \mathbf{a})$, $V_{\phi}(s, \mathbf{a})$ is the critic calculated by minimizing mean square error (MSE) $\mathcal{L}(\phi) = A^2(s, \mathbf{a})$.

Value-based MARL with communication. For value-based MARL, we choose the most popular algorithm QMIX [23] as the basic framework for MARL communication. QMIX learns a decentralized action-value function Q_i for each agent and uses a mixing network to combine these local Q values into a global action-value function Q_{total} . The total loss of QMIX can be denoted as

$$\mathcal{L}_{MARL}^{QMIX} = (r + \gamma \max_{\mathbf{a}'} Q_{total}^-(s', \mathbf{a}') - Q_{total}(s, \mathbf{a}))^2, \quad (2)$$

where r denotes a cooperative reward. The message \mathbf{m}_{-i} is used as the input of $Q_i(o_i, \mathbf{m}_{-i}, a_i)$ in this framework.

4 METHODOLOGY

In this section, we first detail the GIB principle in MARL communication to show its mechanism of saving communication resources. Based on the GIB principle, we propose a novel communication model (CGIBNet). Then, we introduce our method to plug CGIBNet into both policy-based and value-based frameworks.

4.1 GIB principle in MARL communication

Our work focuses on how to learn a communication model to determine what messages to send and whom to address them in bandwidth-restricted settings. In order to simultaneously solve these two problems under a unified framework, we first model multi-agent communication as a graph, where nodes represent agents and edges represent communication channels between agents. Therefore, the communication process can be regarded as the message passing [7] of each node information under the current graph structure. Without loss of generality, we assume that there are L rounds of communication between agents [17] so that the communication graph has L layers. Then the structural representation $m_S^{(l)}$ and the node representation $m_X^{(l)}$ at the l -th layer can be denoted as

$$\begin{aligned} m_S^{(l)} &= \{m_{S,e}^{(l)}, m_{S,e}^{(l)} \in \{0, 1\} \text{ and } e \in \mathcal{E}\} \\ m_X^{(l)} &= \{m_{X,v}^{(l)}, m_{X,v}^{(l)} \in \mathbb{R}^d \text{ and } v \in \mathcal{V}\}, \end{aligned}$$

where \mathcal{E} and \mathcal{V} indicate the valid edge set and the node set at the l -th layer, 0 and 1 indicate the existence of the corresponding edge, d indicates the dimension of the node representation or the number of bits of each node message [32].

Under the above definition, reducing the bandwidth of multi-agent communication is equivalent to compressing the flow of

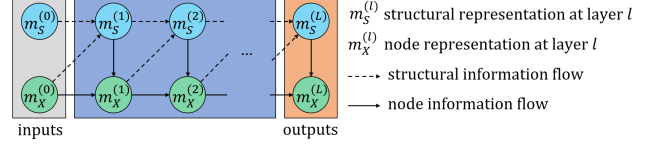


Figure 2: Information flow in the communication graph

structural information and node information in the communication graph. The former leads to fewer edge connections and the latter means that fewer bits can be used to express the whole node information.

Inspired by the information bottleneck (IB) principle [2], which is an information-theoretic principle that extracts the minimal sufficient representation for the target task, we extend it to the graph information bottleneck (GIB) principle in multi-agent communication. Specifically, we introduce two GIB-based criteria to compress the information flow over graph structures.

The first (minimum) criterion is to respectively constrain the structure-level mutual information $I(m_S^{(l-1)}; m_S^{(l)})$ and the node-level mutual information $I(m_X^{(l-1)}; m_X^{(l)})$ between adjacent layers to I_S and I_X . This can obtain concise and compact information flow to reduce communication consumption. Considering that we use message passing [7] to propagate the information in the communication graph, the flow of the structural and node information is coupled as is shown in Figure 2. Thus we rewrite the structure-level and node-level mutual information and denote them as structural information bottleneck $SIB^{(l)}$ and node information bottleneck $XIB^{(l)}$, respectively:

$$\begin{aligned} SIB^{(l)} &= I(m_X^{(l-1)}, m_S^{(l-1)}; m_S^{(l)}) < I_S \\ XIB^{(l)} &= I(m_X^{(l-1)}, m_S^{(l)}; m_X^{(l)}) < I_X. \end{aligned}$$

The second (sufficiency) criterion is to maximize the mutual information between all graph representations and the MARL target to preserve task-related information. Since the communication model is jointly trained with other models, it can be achieved by minimizing the MARL task loss.

According to the above analysis, we formulate the GIB principle in bandwidth-limited communication tasks as

$$\begin{aligned} \min \mathcal{L}_{MARL} \\ \text{s.t. } SIB^{(l)} < I_S \text{ and } XIB^{(l)} < I_X, \forall l \in L, \end{aligned} \quad (3)$$

where $\mathcal{L}_{MARL} \in \{\mathcal{L}_{MARL}^{MAPPO}, \mathcal{L}_{MARL}^{QMIX}\}$ represents the target task loss, I_S and I_X limit the amount of information for structural and node representations to decrease bandwidth usage.

In order to facilitate optimization, we use the Lagrangian function to transform Equation (3) into an unconstrained optimization problem

$$\min \mathcal{L}_{MARL} + \beta_S \sum_{l=1}^L SIB^{(l)} + \beta_X \sum_{l=1}^L XIB^{(l)}, \quad (4)$$

where β_S and β_X represent the Lagrangian multipliers that control the compression strength in the optimization. It is notoriously hard to directly optimize $SIB^{(l)}$ and $XIB^{(l)}$ due to the intractability of

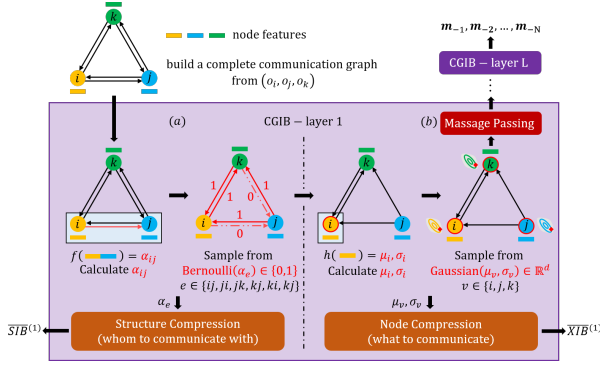


Figure 3: CGIBNet

the mutual information terms. Thus we derive their variational upper bounds as is shown in the following theorem.

THEOREM 1 (UPPER BOUNDS OF $SIB^{(l)}$ AND $XIB^{(l)}$). For arbitrary distributions $r(m_S^{(l)})$ and $r(m_X^{(l)})$,

$$\widehat{SIB}^{(l)} = \mathbb{E}_{m_X^{(l-1)}, m_S^{(l-1)}, m_S^{(l)}} \left[\log \frac{p(m_S^{(l)} | m_X^{(l-1)}, m_S^{(l-1)})}{r(m_S^{(l)})} \right]$$

$$\widehat{XIB}^{(l)} = \mathbb{E}_{m_X^{(l-1)}, m_S^{(l)}, m_X^{(l)}} \left[\log \frac{p(m_X^{(l)} | m_X^{(l-1)}, m_S^{(l)})}{r(m_X^{(l)})} \right].$$

The proof of the theorem is deferred to Supplement A. Then substituting Theorem 2 into Equation (4) obtains an optimization surrogate of communication.

4.2 Instantiating the GIB principle as CGIBNet

In this section, we propose our novel CGIBNet based on the GIB principle, which leverages two information-theoretic regularizers to solve the problem of with whom and what to communicate in bandwidth-limited communication.

The following corollary illustrates the empirical estimation corresponding to Theorem 2 and the components of CGIBNet are implemented based on it.

COROLLARY 1 (EMPIRICAL ESTIMATION OF $\widehat{SIB}^{(l)}$ AND $\widehat{XIB}^{(l)}$).

$$\widehat{SIB}^{(l)} = \sum_{e \in \mathcal{E}} \text{KL} \left(p_e^{(l)}(m_S^{(l)} | m_X^{(l-1)}, m_S^{(l-1)}) || r(m_S^{(l)}) \right)$$

$$\widehat{XIB}^{(l)} = \sum_{v \in \mathcal{V}} \text{KL} \left(p_v^{(l)}(m_X^{(l)} | m_X^{(l-1)}, m_S^{(l)}) || r(m_X^{(l)}) \right).$$

In the corollary, $r(m_S^{(l)})$ and $r(m_X^{(l)})$ are known as the prior structure and the prior node distribution, \mathcal{E} and \mathcal{V} represent the valid edge and valid node set at the l -th layer. The proof of the corollary is deferred to Supplement B.

Structure compression learning. In order to calculate $\widehat{SIB}^{(l)}$ for structural compression, we first focus on the instantiation of $p_e^{(l)}(\cdot)$. Specifically, assume that $m_{X,i}^{(l-1)} \in \mathbb{R}^d$ and $m_{X,j}^{(l-1)} \in \mathbb{R}^d$ are the node representations of node i and node j at the $(l-1)$ -th layer. Then, we suppose the structural representation $m_{S,ij}^{(l)} \in \{0, 1\}$

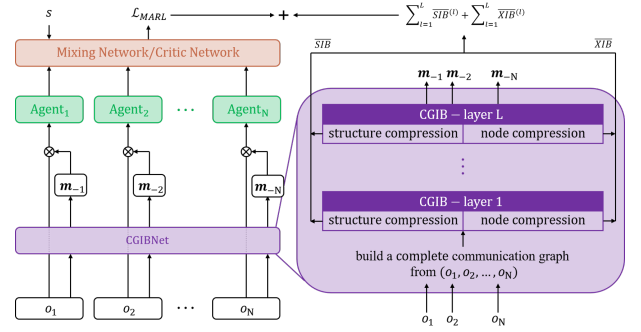


Figure 4: Overall framework of our method

between these two nodes satisfies a Bernoulli distribution, and its parameter $\alpha_{ij}^{(l)}$ is calculated as a link prediction task [34]

$$f([m_{X,i}^{(l-1)}; m_{X,j}^{(l-1)}]) \quad (\text{Figure 3(a)})$$

$$= \text{sigmoid}(f_c([m_{X,i}^{(l-1)}; m_{X,j}^{(l-1)}]))$$

$$= \alpha_{ij}^{(l)},$$

where $[\cdot; \cdot]$ represents vector concatenation and the sigmoid function constrains the output of the link prediction model f_c to the valid range $(0, 1)$. However, it is difficult to back-propagate the gradients if we directly sample $m_{S,ij}^{(l)}$ from Bernoulli($\alpha_{ij}^{(l)}$). Hence we introduce a relaxed Bernoulli distribution, similar to Jang et al. [10], to solve it, as

$$m_{S,ij}^{(l)} \stackrel{\text{iid}}{\sim} \text{RelaxedBernoulli}(\alpha_{ij}^{(l)}, \tau),$$

where $\tau \in (0, \infty)$ is the temperature parameter that controls the approximation. When τ is close to 0, $m_{S,ij}^{(l)}$ is approximately sampled from the set $\{0, 1\}$.

In the forward stage, the structural representation at the l -th layer $m_S^{(l)}$ can be obtained by repeating the process for all valid edges, as is shown in Figure 3(a). In the compression stage, the prior structure distribution $r(m_S^{(l)})$ in Corollary 1 is set to Bernoulli(0.5) as an uninformative prior. Then incorporating $\widehat{SIB}^{(l)}$ into Equation (4) indicates that the structure representation can be compressed by minimizing the KL divergence between the posterior distribution $p_e^{(l)}(\cdot)$ and the prior distribution $r(m_S^{(l)})$.

Node compression learning. Following previous IB methods [2, 21], we present node embedding as a Gaussian random variable and use the reparameterization trick [15] to tackle the gradient blocking problem. That is, the node message at the $(l-1)$ -th layer can be obtained as

$$m_{X,v}^{(l-1)} = \mu_v^{(l-1)} \odot \epsilon + \sigma_v^{(l-1)},$$

where \odot represents the Hadamard product, ϵ is sampled from Gaussian(0, I). The mean $\mu_v^{(l-1)} \in \mathbb{R}^d$ and the variance $\sigma_v^{(l-1)} \in \mathbb{R}^d$ are obtained by the neural network h (Figure 3(b)), and d presents the number of bits. Since $m_S^{(l)}$ has been calculated in the structure learning stage, we can aggregate the information of $m_X^{(l-1)}$ through

message passing. Specifically, assume that node i at the l -th layer needs to receive messages from node j and node k according to $m_S^{(l)}$. Then we have

$$g([m_{X,i}^{(l-1)}; m_{X,j}^{(l-1)}; m_{X,k}^{(l-1)}]) = m_{X,aggre,i}^{(l)},$$

where $m_{X,aggre,i}^{(l)}$ will be used as the output of this layer. In the node compression stage, we set the prior node distribution $r(m_X^{(l)})$ to Gaussian(0, I) as is in the previous work [2, 32]. Then it amounts to minimize the current node information bottleneck of each node message to achieve node compression by Corollary 1.

Despite that all bits are maintained during the training process, we desire to discard some of them to satisfy the communication constraints. An important observation is that the current node information bottleneck of each message bit represents the amount of task-related information. An example is that if the current node information bottleneck of all node bits is 0 under the constraint of the node regularizer in Corollary 1, the posterior Gaussian distribution of all bits is equal to the prior Gaussian distribution Gaussian(0, I). Since there is no difference between these bits, they do not carry any useful information. On the contrary, if the current node information bottleneck of one bit is large while the other bits are 0, it means that this bit is constrained by \mathcal{L}_{MARL} and carries most of the task-related information. Therefore, we can rank all bits according to their node information bottleneck, such that bits with smallest amount of information are discarded after the training process.

4.3 Apply CGIBNet to MARL framework

Some methods (e.g., IC3Net, SchedNet) schedule the structural representations by learning an additional actor so that these methods are not suitable for value-based MARL frameworks. Instead, we model this task as a link prediction task to perform end-to-end training without other restrictions. Therefore, our CGIBNet model can be plugged into both policy-based and value-based MARL frameworks as is shown in Figure 4. For the value-based method, \mathcal{L}_{MARL} in Equation (4) represents $\mathcal{L}_{MARL}^{QMIX}$, and its calculation follows Equation (2). In this case, Agent $_i$ in Figure 4 represents each individual Q_i function, and MixingNetwork Q_{tot} is used to aggregate global information. Similarly, for the policy-based method, \mathcal{L}_{MARL} in Equation (4) represents \mathcal{L}_{MARL}^{AC} , and its calculation follows Equation (??). In this case, Agent $_i$ in Figure 4 represents each individual actor π_i , and CriticNetwork V is used to aggregate global information. See Supplement C for the pseudo-code of CGIBNet.

5 EXPERIMENTS

In this section, we evaluate CGIBNet in two environments with bandwidth-constrained communication. The first one is Traffic Control, where we use a policy-based MARL framework (i.e., Actor-Critic) for training. The second is the StarCraftII [25], where we use a value-based MARL framework (i.e., QMIX) for training.

5.1 Evaluation Metric

To better illustrate our experiments, we first introduce two metrics to measure the compression of bandwidth.

Structure Compression Ratio (SCR). This metric refers to Kim et al. [13]. It focuses on the density of edge connections in

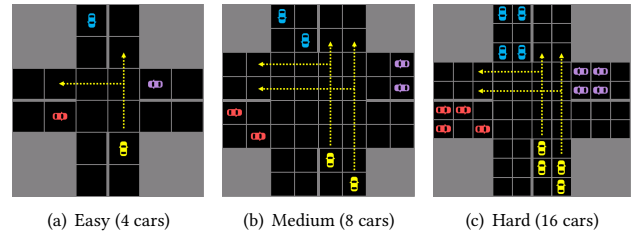


Figure 5: Traffic control environment

the communication graph and assumes the message bits transmitted by each edge are consistent. Formally, let $N_{e,complete}$ and $N_{e,compressed}$ denote the number of edges of the communication graph structure without and with structure compression, respectively. Then, SCR is defined as $N_{e,complete} - N_{e,compressed} / N_{e,complete} \times 100\%$.

Message Compression Ratio (MCR). This metric refers to Wang et al. [32]. It focuses on the message bits in the communication graph. The insight behind MCR is that the length of the message sent by each agent should be adaptive and various in different situations, and few node message bits can compress sufficient information for effective communication. However, the agent network requires the input of fixed-length messages. Therefore, we introduce a binary mask for each message bit to simulate controllable limited bandwidth. Formally, let $N_{m,complete}$ denote the message bits without compression and $N_{m,compressed}$ denotes the unmasked message bits with compression. Then, MCR is defined as $N_{m,complete} - N_{m,compressed} / N_{m,complete} \times 100\%$. We can find MCR can cover all cases of SCR according to their definition, thus MCR can reflect the degree of both structure and node compression. In practice, the masking strategy is based on the importance of each message bit. For methods that include node compression (e.g., NDQ, IMAC, CGIBNet), as mentioned in Section 4.2, we sort the message distributions in ascending order according to their current node information bottleneck, and mask them accordingly; for attention-based method (e.g., G2A), we mask their message bits according to attention weights; for other methods (e.g., IC3Net), we mask their message bits according to their absolute value. See Supplement D for calculation details.

5.2 Traffic Control

Environment description. As is shown in Figure 5, each car is modeled as an agent, and they should learn a good cooperative policy to ensure that they can quickly pass through the junction with as few collisions as possible. The collision only affects the reward of the corresponding agent without changing the environment simulation. At the start of the episode, each car needs to randomly initialize a starting position near the entrance and randomly select one of the two possible routes. The termination condition of the environment is that all cars exit the junction or exceed the maximum timestep (20, 40, 60 for easy, medium and hard maps respectively). For each car, the local observation contains its location and assigned route id. The action is a discrete number $a \in \{0, 1\}$, where 0 represents stop and 1 represents move one step forward. The

Map	Easy				
	SCR	R under the left SCR	R under MCR=50%	R under MCR=75%	R under MCR=100%
MAPPO+IC3Net	10%	12.5	-38.3	-103.4	-205.5
MAPPO+G2A	7%	16.2	-25.7	-94.0	-196.4
MAPPO+NDQ	0%	13.0	3.1	0.6	-289.8
MAPPO+SchedIMAC	0%	12.1	4.5	1.5	-277.4
MAPPO+CGIBNet	17%	14.8	6.1	3.9	-269.2
Map	Medium				
Evaluation Mode	SCR	R under the left SCR	R under MCR=50%	R under MCR=75%	R under MCR=100%
MAPPO+IC3Net	21%	14.6	-53.5	-298.9	-531.2
MAPPO+G2A	18%	24.1	-40.1	-244.2	-549.3
MAPPO+NDQ	0%	2.8	-9.8	-18.2	-666.0
MAPPO+SchedIMAC	29%	14.2	3.5	-2.6	-604.7
MAPPO+CGIBNet	30%	19.4	13.2	9.9	-642.1
Map	Hard				
Evaluation Mode	SCR	R under the left SCR	R under MCR=50%	R under MCR=75%	R under MCR=100%
MAPPO+IC3Net	20%	-1254.0	-2064.1	-2946.3	-4638.3
MAPPO+G2A	19%	-1108.3	-1943.0	-2857.4	-3835.1
MAPPO+NDQ	0%	-2529.6	-2684.2	-2871.6	-5934.0
MAPPO+SchedIMAC	27%	-1484.4	-1556.9	-1773.6	-5421.4
MAPPO+CGIBNet	28%	-1195.8	-1231.6	-1289.0	-6284.7

Table 1: Experimental results in different restrictions on traffic control. ‘R’ indicates cumulative reward per episode. SCR= $p\%$ indicates that the available communication channels are compressed by $p\%$. MCR= $p\%$ indicates that the available message bits are compressed by $p\%$.

reward consists of three parts: timestep penalty $R_{tp,i} = -1$, collision penalty $R_{cp,i} = -100$ and exit bouns $R_{eb,i} = 30$. Thus the shared total reward at timestep t is $R_{tot} = \sum_i^N (t \times R_{tp,i} + R_{cp,i} + R_{eb,i})$. The number of grids and cars on each map is consistent with Figure 5. See Supplement E.1 for more details.

Experimental setups. In this environment, we modify MAPPO [?] algorithm as the training framework and compare CGIBNet with various baselines, including IC3Net [27], G2A [16], SchedNet [13], NDQ [32] and IMAC [31], where IC3Net and G2A only schedule the edge connections in the communication graph; SchedNet uses a predefined number to fix the scale of agents’ communication group, and this process compresses the structure information to a certain extent; NDQ and IMAC only compress node information while ignores structural information. Since SchedNet and IMAC learn a scheduler in a similar way and they only consider one of structure compression or node compression, we combine these two methods to construct a strong baseline, which is called SchedIMAC. For experimental hyperparameters, we set the predefined limited number in SchedIMAC to 3, 5, 11 in easy, medium and hard maps respectively. For our method, we set structural Lagrangian multiplier β_S and node Lagrangian multiplier β_X to 0.1 and 0.001 respectively. More experimental details are elaborated in Supplement F.

Results. Table 1 shows the average results of 5 experiments on traffic control tasks. The ‘SCR’ related results are obtained by standard evaluation without any restrictions, which indicates the ability of the corresponding model to compress the structure information in the communication graph. The ‘MCR’ related results are obtained by limiting available message bits during the evaluation process, which ensures that the message compression strength of all methods is consistent so as to make a fair comparison.

According to the result of structural compression, NDQ is the only method to communicate using a fully connected graph (*i.e.*, SCR=0%) and it achieves poor performance on complex maps, which indicates that traffic control task relies on scheduling with whom to communicate, otherwise too much redundant information will

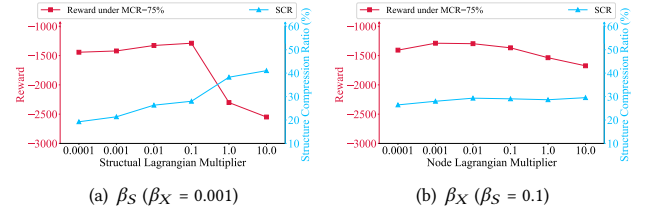


Figure 6: The results on hard map w.r.t. different β_S and β_X

lead to multi-agent miscoordination. Interestingly, we find that the performance of CGIBNet is better than IC3Net even though CGIBNet has a larger SCR, which indicates our structural regularizer can effectively cut redundant edge connections in the communication graph. Additionally, CGIBNet and SchedIMAC are both structural compression methods with similar SCR on medium and hard maps, but the performance of CGIBNet is much better than that of SchedIMAC, which further shows the superiority of CGIBNet. Although G2A achieves the best performance thanks to its attention mechanism, it needs to occupy more bandwidth than CGIBNet.

According to the result of message compression, the performance of IC3Net and G2A has significantly reduced under MCR=50% and MCR=75%. This is because these methods do not compress the node information, leading to a small number of bits that cannot express sufficient content for communication. Therefore, these communication models are not suitable for scenarios with severe bandwidth limitations. The performance of CGIBNet surpasses all other methods under MCR=50% and MCR=75% while maintaining a tolerable degradation compared to the standard evaluation, especially for hard maps. This indicates CGIBNet can effectively determine what messages to send and whom to address them so that just a few message bits are enough for communication. In addition, the performance of all methods decreases drastically when all communication channels are closed (*i.e.*, MCR=100%), proving that the success of our method comes from the compressive communication graph instead of implicit coordination strategies are learned.

The influence of β_S and β_X on CGIBNet. From the optimization perspective, Lagrangian multipliers β_S and β_X in Equation (4) control the structure and node compression strength respectively. Figure 6 shows that as the compression strength increases (*i.e.*, β_S and β_X become larger), the performance of our model under MCR=75% will gradually rise. However, when they exceed a certain critical value, the information distortion caused by over-compression will lead to performance degradation or even collapse. *e.g.*, SCR exceeds 40% in Figure 6(a). Therefore, we recommend setting β_S to $10^{-2} \sim 10^{-1}$ and β_X to $10^{-3} \sim 10^{-2}$.

5.3 StarCraftII

Environment description. StarCraftII micromanagement [25] is a real-time strategy game and its built-in maps are widely used to study the credit assignment problem [23] in the MARL community. Recently, Wang et al. [32] introduces 4 new maps to explore the communication mechanism in value-based MARL frameworks. Specifically, these maps include 3b_vs_1h1m, 1o2r_vs_4r, 5z_vs_1ul and 1o10b_vs_1r. The number and letter on the left of ‘vs’ indicate

Map		3b_vs_1h1m				
Evaluation Mode	SCR	WR under the left SCR	WR under MCR=50%	WR under MCR=75%	WR under MCR=100%	
QMIX+G2A	12%	74.9%	51.2%	31.9%	11.2%	
QMIX+NDQ	0%	78.9%	73.2%	69.0%	2.1%	
QMIX+IMAC	0%	77.2%	72.9%	67.9%	1.8%	
QMIX+CGIBNet	20%	78.0%	74.5%	69.4%	3.2%	
Map		1o2r_vs_4r				
Evaluation Mode	SCR	WR under the left SCR	WR under MCR=50%	WR under MCR=75%	WR under MCR=100%	
QMIX+G2A	15%	82.7%	46.4%	38.3%	18.1%	
QMIX+NDQ	0%	81.9%	75.8%	72.1%	25.2%	
QMIX+IMAC	0%	81.6%	74.3%	71.2%	20.6%	
QMIX+CGIBNet	26%	82.2%	78.3%	76.6%	16.2%	
Map		5z_vs_1ul				
Evaluation Mode	SCR	WR under the left SCR	WR under MCR=50%	WR under MCR=75%	WR under MCR=100%	
QMIX+G2A	21%	63.6%	31.2%	20.6%	23.8%	
QMIX+NDQ	0%	62.4%	59.8%	56.4%	31.6%	
QMIX+IMAC	0%	61.8%	57.6%	53.3%	37.7%	
QMIX+CGIBNet	37%	64.7%	63.3%	62.1%	34.7%	
Map		1o10b_vs_1r				
Evaluation Mode	SCR	WR under the left SCR	WR under MCR=50%	WR under MCR=75%	WR under MCR=100%	
QMIX+G2A	26%	84.5%	59.5%	39.8%	19.6%	
QMIX+NDQ	0%	78.8%	74.4%	70.5%	10.4%	
QMIX+IMAC	0%	77.3%	69.8%	67.1%	7.1%	
QMIX+CGIBNet	44%	83.6%	81.0%	79.6%	5.5%	

Table 2: Experimental results in different restrictions on StarCraftII. ‘WR’ indicates the average win rate. SCR= $p\%$ indicates that the available communication channels are compressed by $p\%$. MCR= $p\%$ indicates that the available message bits are compressed by $p\%$.

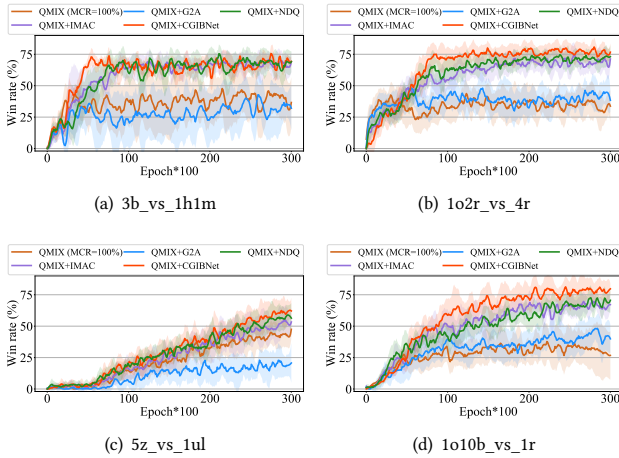


Figure 7: The StarCraftII training curves under MCR=75%

the number and type of agents we trained, and the right is the information of built-in agents. For the 3b_vs_1h1m map, 3 Banelings need to reach the designated location and attack the enemy at the same time. For 1o2r_vs_4r and 1o10b_vs_1r map, 1 Overseer needs to continuously provide the enemy’s vision to guide the allied forces. For the 5z_vs_1ul map, 5 Zealots need to cooperate and communicate frequently to defeat a powerful Ultralisk. More details can be found in Supplement E.2.

Experimental setups. In this environment, we choose QMIX [23], a well-known value-based method, as the training framework. Since IC3Net and SchedNet need to learn an additional actor as a scheduler, they are not suitable for extension into value-based frameworks. Therefore, we mainly compare CGIBNet with G2A,

NDQ and IMAC. For our method, we set β_S and β_X to 0.1 and 0.001 respectively. More experimental details are elaborated in Supplement F.

Results. Table 2 shows the average results of 5 experiments on StarCraftII. For all maps, the result is similar to that of traffic control. Specifically, CGIBNet can maximally reduce the communication channels between agents (*i.e.*, large SCR) and preserve sufficient information for decision-making. Also, it maintains its powerful ability under different MCR evaluations, especially for large-scale multi-agent settings, which verifies the superiority of our method under the value-based framework. Figure 7 demonstrates the curve of the win rate under MCR=75% during the training phase. We can find the convergence speed of CGIBNet is faster than other methods. This shows that our method inherits the advantages of the IB theory [26], that is, the compact structure representation and node representation obtained by our method can improve the utilization of each sample. In addition, the poor performance of vanilla QMIX (MCR=100%) in Figure 7 verifies the necessity of communication on these 4 maps.

6 CONCLUSION

In this paper, we focus on how to learn a communication model to determine each agent is communicating what message and to whom in bandwidth-restricted settings. By modeling multi-agent communication as a directed complete graph, we propose our novel CGIBNet, which leverages the graph information bottleneck principle to compress the flow of node information over the graph structure while maximally preserve information for decision-making. We plug CGIBNet into both policy-based and value-based frameworks and verify them in Traffic Control and StarCraftII respectively. Empirical results show the superiority of CGIBNet under bandwidth-restricted settings, especially for large-scale multi-agent systems.

REFERENCES

- [1] S Ahilan and P Dayan. 2021. Correcting Experience Replay for Multi-Agent Communication. In *ICLR*.
- [2] Alexander A Alemi, Ian Fischer, Joshua V Dillon, and Kevin Murphy. 2017. Deep variational information bottleneck. In *ICLR*.
- [3] Abhishek Das, Théophile Gervet, Joshua Romoff, Dhruv Batra, Devi Parikh, Mike Rabbat, and Joelle Pineau. 2019. Tarmac: Targeted multi-agent communication. In *ICML*.
- [4] Ali Dorri, Salil S Kanhere, and Raja Jurdak. 2018. Multi-agent systems: A survey. *Ieee Access* 6 (2018), 28573–28593.
- [5] Yali Du, Yifan Zhao, Meng Fang, Jun Wang, Gangyan Xu, and Haifeng Zhang. 2020. Learning Predictive Communication by Imagination in Networked System Control. (2020).
- [6] Jakob N Foerster, Yannis M Assael, Nando de Freitas, and Shimon Whiteson. 2016. Learning to communicate with deep multi-agent reinforcement learning. In *NeurIPS*.
- [7] Justin Gilmer, Samuel S Schoenholz, Patrick F Riley, Oriol Vinyals, and George E Dahl. 2017. Neural message passing for quantum chemistry. In *ICML*.
- [8] Maximilian Hüttenrauch, Sosic Adrian, Gerhard Neumann, et al. 2019. Deep reinforcement learning for swarm systems. *Journal of Machine Learning Research* 20, 54 (2019), 1–31.
- [9] Maximilian Igl, Kamil Ciosek, Yingzhen Li, Sebastian Tschiatschek, Cheng Zhang, Sam Devlin, and Katja Hofmann. 2019. Generalization in Reinforcement Learning with Selective Noise Injection and Information Bottleneck. In *NeurIPS*.
- [10] Eric Jang, Shixiang Gu, and Ben Poole. 2017. Categorical reparameterization with gumbel-softmax. In *ICLR*.
- [11] Jiechuan Jiang, Chen Dun, Tiejun Huang, and Zongqing Lu. 2020. Graph Convolutional Reinforcement Learning. In *ICLR*.
- [12] Jiechuan Jiang and Zongqing Lu. 2018. Learning Attentional Communication for Multi-Agent Cooperation. In *NeurIPS*.
- [13] Daewoo Kim, Sangwoo Moon, David Hostallero, Wan Ju Kang, Taeyoung Lee, Kyunghwan Son, and Yung Yi. 2019. Learning to Schedule Communication in

- Multi-agent Reinforcement Learning. In *ICLR*.
- [14] Woojun Kim, Jongeui Park, and Youngchul Sung. 2021. Communication in Multi-Agent Reinforcement Learning: Intention Sharing. In *ICLR*.
 - [15] Diederik P Kingma and Max Welling. 2014. Auto-encoding variational bayes. In *ICLR*.
 - [16] Yong Liu, Weixun Wang, Yujing Hu, Jianye Hao, Xingguo Chen, and Yang Gao. 2020. Multi-agent game abstraction via graph attention neural network. In *AAAI*.
 - [17] Georgios Papoudakis, Filippos Christianos, Arrasy Rahman, and Stefano V Albrecht. 2019. Dealing with non-stationarity in multi-agent deep reinforcement learning. *arXiv preprint arXiv:1906.04737* (2019).
 - [18] Peng Peng, Ying Wen, Yaodong Yang, Quan Yuan, Zhenkun Tang, Haitao Long, and Jun Wang. 2017. Multiagent bidirectionally-coordinated nets: Emergence of human-level coordination in learning to play starcraft combat games. *arXiv:1703.10069* (2017).
 - [19] Xue Bin Peng, Angjoo Kanazawa, Sam Toyer, Pieter Abbeel, and Sergey Levine. 2018. Variational Discriminator Bottleneck: Improving Imitation Learning, Inverse RL, and GANs by Constraining Information Flow. In *ICLR*.
 - [20] Emanuele Pesse and Giovanni Montana. 2020. Improving coordination in small-scale multi-agent deep reinforcement learning through memory-driven communication. *Machine Learning* (2020), 1–21.
 - [21] Kaizhi Qian, Yang Zhang, Shiyu Chang, Mark Hasegawa-Johnson, and David Cox. 2020. Unsupervised speech decomposition via triple information bottleneck. In *ICML*.
 - [22] M Rangwala and R Williams. 2020. Learning Multi-Agent Communication through Structured Attentive Reasoning. In *NeurIPS*.
 - [23] Tabish Rashid, Mikayel Samvelyan, Christian Schroeder, Gregory Farquhar, Jakob Foerster, and Shimon Whiteson. 2018. Qmix: Monotonic value function factorization for deep multi-agent reinforcement learning. In *ICML*.
 - [24] Ahmad EL Sallab, Mohammed Abdou, Etienne Perot, and Senthil Yogamani. 2017. Deep reinforcement learning framework for autonomous driving. *Electronic Imaging 2017*, 19 (2017), 70–76.
 - [25] Mikayel Samvelyan, Tabish Rashid, Christian Schröder de Witt, Gregory Farquhar, Nantas Nardelli, Tim GJ Rudner, Chia-Man Hung, Philip HS Torr, Jakob N Foerster, and Shimon Whiteson. 2019. The StarCraft Multi-Agent Challenge. In *AAMAS*.
 - [26] Ohad Shamir, Sivan Sabato, and Naftali Tishby. 2010. Learning and generalization with the information bottleneck. *Theoretical Computer Science* 411, 29-30 (2010), 2696–2711.
 - [27] Amanpreet Singh, Tushar Jain, and Sainbayar Sukhbaatar. 2018. Learning when to Communicate at Scale in Multiagent Cooperative and Competitive Tasks. In *ICLR*.
 - [28] Sainbayar Sukhbaatar, Arthur Szlam, and Rob Fergus. 2016. Learning multiagent communication with backpropagation. In *NeurIPS*.
 - [29] Richard S Sutton, David A McAllester, Satinder P Singh, and Yishay Mansour. 2000. Policy gradient methods for reinforcement learning with function approximation. In *NeurIPS*.
 - [30] Naftali Tishby, Fernando C Pereira, and William Bialek. 1999. The information bottleneck method. In *Proc. 37th Annual Allerton Conference on Communications, Control and Computing, 1999*.
 - [31] Rundong Wang, Xu He, Runsheng Yu, Wei Qiu, Bo An, and Zinovi Rabinovich. 2020. Learning efficient multi-agent communication: An information bottleneck approach. In *ICML*.
 - [32] Tonghan Wang, Jianhao Wang, Chongyi Zheng, and Chongjie Zhang. 2020. Learning Nearly Decomposable Value Functions Via Communication Minimization. In *ICLR*.
 - [33] Tailin Wu, Hongyu Ren, Pan Li, and Jure Leskovec. 2020. Graph Information Bottleneck. In *NeurIPS*.
 - [34] Muhan Zhang and Yixin Chen. 2018. Link prediction based on graph neural networks. In *NeurIPS*.

7 SUPPLEMENT

7.1 A. Proof for Theorem 1

THEOREM 2 (UPPER BOUNDS OF $SIB^{(l)}$ AND $XIB^{(l)}$). For arbitrary distributions $r(m_S^{(l)})$ and $r(m_X^{(l)})$,

$$\begin{aligned}\widehat{SIB}^{(l)} &= \mathbb{E}_{m_X^{(l-1)}, m_S^{(l-1)}, m_S^{(l)}} \left[\log \frac{p(m_S^{(l)} | m_X^{(l-1)}, m_S^{(l-1)})}{r(m_S^{(l)})} \right] \\ \widehat{XIB}^{(l)} &= \mathbb{E}_{m_X^{(l-1)}, m_S^{(l)}, m_X^{(l)}} \left[\log \frac{p(m_X^{(l)} | m_X^{(l-1)}, m_S^{(l)})}{r(m_X^{(l)})} \right].\end{aligned}$$

Proof. We first derive the structural information bottleneck $SIB^{(l)}$ as

$$\begin{aligned}SIB^{(l)} &= I(m_X^{(l-1)}, m_S^{(l-1)}; m_S^{(l)}) \\ &= \int_{m_X^{(l-1)}} \int_{m_S^{(l-1)}} \int_{m_S^{(l)}} p(m_X^{(l-1)}, m_S^{(l-1)}, m_S^{(l)}) \log \left(\frac{p(m_X^{(l-1)}, m_S^{(l-1)}, m_S^{(l)})}{p(m_X^{(l-1)}, m_S^{(l-1)}) p(m_S^{(l)})} \right) dm_X^{(l-1)} dm_S^{(l-1)} dm_S^{(l)} \\ &= \int_{m_X^{(l-1)}} \int_{m_S^{(l-1)}} \int_{m_S^{(l)}} p(m_X^{(l-1)}, m_S^{(l-1)}, m_S^{(l)}) \log \left(\frac{p(m_S^{(l)} | m_X^{(l-1)}, m_S^{(l-1)}) p(m_X^{(l-1)}, m_S^{(l-1)})}{p(m_X^{(l-1)}, m_S^{(l-1)}) p(m_S^{(l)})} \right) dm_X^{(l-1)} dm_S^{(l-1)} dm_S^{(l)} \\ &= \int_{m_X^{(l-1)}} \int_{m_S^{(l-1)}} \int_{m_S^{(l)}} p(m_X^{(l-1)}, m_S^{(l-1)}, m_S^{(l)}) \log \left(\frac{p(m_S^{(l)} | m_X^{(l-1)}, m_S^{(l-1)})}{p(m_S^{(l)})} \right) dm_X^{(l-1)} dm_S^{(l-1)} dm_S^{(l)} \quad (5) \\ &= \int_{m_X^{(l-1)}} \int_{m_S^{(l-1)}} \int_{m_S^{(l)}} p(m_X^{(l-1)}, m_S^{(l-1)}, m_S^{(l)}) \log p(m_S^{(l)} | m_X^{(l-1)}, m_S^{(l-1)}) dm_X^{(l-1)} dm_S^{(l-1)} dm_S^{(l)} \\ &\quad - \int_{m_X^{(l-1)}} \int_{m_S^{(l-1)}} \int_{m_S^{(l)}} p(m_X^{(l-1)}, m_S^{(l-1)}, m_S^{(l)}) \log p(m_S^{(l)}) dm_X^{(l-1)} dm_S^{(l-1)} dm_S^{(l)} \\ &= \int_{m_X^{(l-1)}} \int_{m_S^{(l-1)}} \int_{m_S^{(l)}} p(m_X^{(l-1)}, m_S^{(l-1)}, m_S^{(l)}) \log p(m_S^{(l)} | m_X^{(l-1)}, m_S^{(l-1)}) dm_X^{(l-1)} dm_S^{(l-1)} dm_S^{(l)} \\ &\quad - \int_{m_S^{(l)}} p(m_S^{(l)}) \log p(m_S^{(l)}) dm_S^{(l)}.\end{aligned}$$

However, it is difficult to compute the marginal distribution $p(m_S^{(l)})$, so let $r(m_S^{(l)})$ be a variational approximation to this marginal. Then we have

$$\begin{aligned}KL \left[p(m_S^{(l)}), r(m_S^{(l)}) \right] &\geq 0 \\ - \int_{m_S^{(l)}} p(m_S^{(l)}) \log p(m_S^{(l)}) dm_S^{(l)} &\leq - \int_{m_S^{(l)}} r(m_S^{(l)}) \log r(m_S^{(l)}) dm_S^{(l)}.\end{aligned} \quad (6)$$

Substituting Equation (6) into Equation (5), we have

$$\begin{aligned}SIB^{(l)} &\leq \int_{m_X^{(l-1)}} \int_{m_S^{(l-1)}} \int_{m_S^{(l)}} p(m_X^{(l-1)}, m_S^{(l-1)}, m_S^{(l)}) \log p(m_S^{(l)} | m_X^{(l-1)}, m_S^{(l-1)}) dm_X^{(l-1)} dm_S^{(l-1)} dm_S^{(l)} \\ &\quad - \int_{m_S^{(l)}} r(m_S^{(l)}) \log r(m_S^{(l)}) dm_S^{(l)} \\ &\leq \int_{m_X^{(l-1)}} \int_{m_S^{(l-1)}} \int_{m_S^{(l)}} p(m_X^{(l-1)}, m_S^{(l-1)}, m_S^{(l)}) \log \left(\frac{p(m_S^{(l)} | m_X^{(l-1)}, m_S^{(l-1)})}{r(m_S^{(l)})} \right) dm_X^{(l-1)} dm_S^{(l-1)} dm_S^{(l)} \\ &\leq \mathbb{E}_{m_X^{(l-1)}, m_S^{(l-1)}, m_S^{(l)} \sim p(m_X^{(l-1)}, m_S^{(l-1)}, m_S^{(l)})} \left[\frac{p(m_S^{(l)} | m_X^{(l-1)}, m_S^{(l-1)})}{r(m_S^{(l)})} \right].\end{aligned}$$

Thus the upper bound of $SIB^{(l)}$ can be written as

$$\widehat{SIB}^{(l)} = \mathbb{E}_{m_X^{(l-1)}, m_S^{(l-1)}, m_S^{(l)} \sim p(m_X^{(l-1)}, m_S^{(l-1)}, m_S^{(l)})} \left[\frac{p(m_S^{(l)} | m_X^{(l-1)}, m_S^{(l-1)})}{r(m_S^{(l)})} \right].$$

Similarly, we can get the upper bound of $XIB^{(l)}$ by replacing the above variables $m_S^{(l-1)} \rightarrow m_S^{(l)}$ and $m_S^{(l)} \rightarrow m_X^{(l)}$, then we have

$$\widehat{XIB}^{(l)} = \mathbb{E}_{m_X^{(l-1)}, m_S^{(l)}, m_X^{(l)} \sim p(m_X^{(l-1)}, m_S^{(l)}, m_X^{(l)})} \left[\log \frac{p(m_X^{(l)} | m_X^{(l-1)}, m_S^{(l)})}{r(m_X^{(l)})} \right].$$

7.2 B. Proof for Corollary 1

COROLLARY 2 (EMPIRICAL ESTIMATION OF $\widehat{SIB}^{(l)}$ AND $\widehat{XIB}^{(l)}$).

$$\begin{aligned} \overline{SIB}^{(l)} &= \sum_{e \in \mathcal{E}} \text{KL} \left(p_e^{(l)}(m_S^{(l)} | m_X^{(l-1)}, m_S^{(l-1)}) || r(m_S^{(l)}) \right) \\ \overline{XIB}^{(l)} &= \sum_{v \in \mathcal{V}} \text{KL} \left(p_v^{(l)}(m_X^{(l)} | m_X^{(l-1)}, m_S^{(l)}) || r(m_X^{(l)}) \right). \end{aligned}$$

Proof. According to Theorem 2, we can obtain the upper bounds $\widehat{SIB}^{(l)}$ and $\widehat{XIB}^{(l)}$. Based on them, we first derive the empirical estimate of $\overline{SIB}^{(l)}$ as

$$\begin{aligned} \widehat{SIB}^{(l)} &= \mathbb{E}_{m_X^{(l-1)}, m_S^{(l-1)}, m_S^{(l)} \sim p(m_X^{(l-1)}, m_S^{(l-1)}, m_S^{(l)})} \left[\frac{p(m_S^{(l)} | m_X^{(l-1)}, m_S^{(l-1)})}{r(m_S^{(l)})} \right] \\ &= \int_{m_X^{(l-1)}} \int_{m_S^{(l-1)}} \int_{m_S^{(l)}} p(m_X^{(l-1)}, m_S^{(l-1)}, m_S^{(l)}) \log \left(\frac{p(m_S^{(l)} | m_X^{(l-1)}, m_S^{(l-1)})}{r(m_S^{(l)})} \right) dm_X^{(l-1)} dm_S^{(l-1)} dm_S^{(l)} \\ &= \int_{m_X^{(l-1)}} \int_{m_S^{(l-1)}} \int_{m_S^{(l)}} p(m_X^{(l-1)}, m_S^{(l-1)}) p(m_S^{(l)} | m_X^{(l-1)}, m_S^{(l-1)}) \log \left(\frac{p(m_S^{(l)} | m_X^{(l-1)}, m_S^{(l-1)})}{r(m_S^{(l)})} \right) dm_X^{(l-1)} dm_S^{(l-1)} dm_S^{(l)} \\ &= \int_{m_X^{(l-1)}} \int_{m_S^{(l-1)}} \int_{m_S^{(l)}} p(m_X^{(l-1)}, m_S^{(l-1)}) \text{KL} \left[p(m_S^{(l)} | m_X^{(l-1)}, m_S^{(l-1)}) || r(m_S^{(l)}) \right] dm_X^{(l-1)} dm_S^{(l-1)} dm_S^{(l)} \\ &= \mathbb{E}_{m_X^{(l-1)}, m_S^{(l-1)} \sim p(m_X^{(l-1)}, m_S^{(l-1)})} \text{KL} \left[p(m_S^{(l)} | m_X^{(l-1)}, m_S^{(l-1)}) || r(m_S^{(l)}) \right]. \end{aligned} \tag{7}$$

In order to calculate the KL divergence in Equation (7), we need to sample $m_X^{(l-1)}$ and $m_S^{(l-1)}$ at the $(l-1)$ -th layer to calculate the valid structural representation $m_S^{(l)}$ at the l -th layer. After $m_S^{(l)}$ is obtained, the empirical estimation of $SIB^{(l)}$ can be denoted as

$$\overline{SIB}^{(l)} = \sum_{e \in \mathcal{E}} \text{KL} \left(p_e^{(l)}(m_S^{(l)} | m_X^{(l-1)}, m_S^{(l-1)}) || r(m_S^{(l)}) \right),$$

where \mathcal{E} represents the valid edge set at the l -th layer. Similarly, we can get the empirical estimation of $XIB^{(l)}$ by replacing the above variables $m_S^{(l-1)} \rightarrow m_S^{(l)}$ and $m_S^{(l)} \rightarrow m_X^{(l)}$, then we have

$$\overline{XIB}^{(l)} = \sum_{v \in \mathcal{V}} \text{KL} \left(p_v^{(l)}(m_X^{(l)} | m_X^{(l-1)}, m_S^{(l)}) || r(m_X^{(l)}) \right),$$

where \mathcal{V} represents the valid node set at the l -th layer.

7.3 C. The pseudo-code of CGIBNet

Algorithm 1 Communicative Graph information Bottleneck Network (CGIBNet)

Inputs: Local observation of each agent (o_1, o_2, \dots, o_N), alive mask of each agent (al_1, al_2, \dots, al_N)

Neural networks: Edge network f , node network h , aggregation network g

Hyperparameters: The number of communication rounds L , the temperature coefficient in relaxed Bernoulli distribution τ

Outputs: The message received by each agent ($\mathbf{m}_{-1}, \mathbf{m}_{-2}, \dots, \mathbf{m}_{-N}$), structural information bottleneck \overline{SIB} , node information bottleneck \overline{XIB}

```

1: Let the edge set  $\mathcal{E} = \{m_{S,ij} = 1, 1 \leq i, j \leq N\}$ , the node set  $\mathcal{V} = \{m_{X,i} = o_i, 1 \leq i \leq N\}$ ,  $\overline{SIB} = 0$ ,  $\overline{XIB} = 0$ 
2: # Only alive agents can participate in the communication process
3: for  $n = 1, 2, \dots, N$  do
4:   if  $al_n = 0$  then
5:     Change the valid edge set  $m_{S,nk} = 0$  and  $m_{S,kn} = 0$  ( $1 \leq k \leq N$ )
6:     Change the valid node set  $m_{X,n} = \emptyset$ 
7:   end if
8: end for
9: # Communication process
10: for  $l = 1, 2, \dots, L$  do
11:   # Structure compression learning
12:   for  $m_{S,ij} \in \mathcal{E}$  do
13:     if  $m_{S,ij} = 1$  then
14:       Calculate the parameter of the Bernoulli distribution  $\alpha_{ij} = f(m_{X,i}, m_{X,j})$ 
15:       Use  $\alpha_{ij}$  to calculate  $\overline{SIB}_{ij}$  according to Corollary 1
16:       Add all structural information bottlenecks together for gradient propagation  $\overline{SIB} = \overline{SIB} + \overline{SIB}_{ij}$ 
17:       Sample new  $m_{S,ij} \stackrel{\text{iid}}{\sim} \text{RelaxedBernoulli}(\alpha_{ij}, \tau)$ 
18:     end if
19:   end for
20:   # Node compression learning
21:   for  $m_{X,i} \in \mathcal{V}$  do
22:     if  $m_{X,i} \neq \emptyset$  then
23:       Calculate the parameters of the Gaussian distribution  $\mu_i, \sigma_i = h(m_{X,i})$ 
24:       Use  $\mu_i, \sigma_i$  to calculate  $\overline{XIB}_i$  according to Corollary 1
25:       Add all node information bottlenecks together for gradient propagation  $\overline{XIB} = \overline{XIB} + \overline{XIB}_i$ 
26:       Sample new  $m_{X,i} \stackrel{\text{iid}}{\sim} \text{Gaussian}(\mu_i, \sigma_i)$ 
27:     end if
28:   end for
29:   # Message aggregation
30:   for  $m_{X,i} \in \mathcal{V}$  do
31:     Concatenate all current messages together  $cur\_concat = \text{concat}(m_{X,1}, \dots, m_{X,N})$ 
32:     Mask out the corresponding positions that do not send messages to agent  $i$  ( $m_{S,ki} = 0, (1 \leq k \leq N)$ ) in  $cur\_concat$ 
33:     Aggregate messages sent to agent  $i$ , that is,  $m_{X,i} = g(cur\_concat)$ 
34:   end for
35: end for
36: Assign the aggregated messages to the output  $(\mathbf{m}_{-1}, \mathbf{m}_{-2}, \dots, \mathbf{m}_{-N}) = (m_{X,1}, m_{X,2}, \dots, m_{X,N})$ 
37: return  $(\mathbf{m}_{-1}, \mathbf{m}_{-2}, \dots, \mathbf{m}_{-N}), \overline{SIB}, \overline{XIB}$ 

```

7.4 D. Calculation details about Structure Compression Ratio (SCR) and Message Compression Ratio (MCR)

Structure Compression Ratio (SCR). Recall the definition of SCR mentioned in Section 5.1. Let $N_{e,complete}$ and $N_{e,compressed}$ denote the number of edges of the communication graph structure without and with structure compression, respectively. Then, SCR is calculated as $N_{e,complete} - N_{e,compressed} / N_{e,compressed} \times 100\%$.

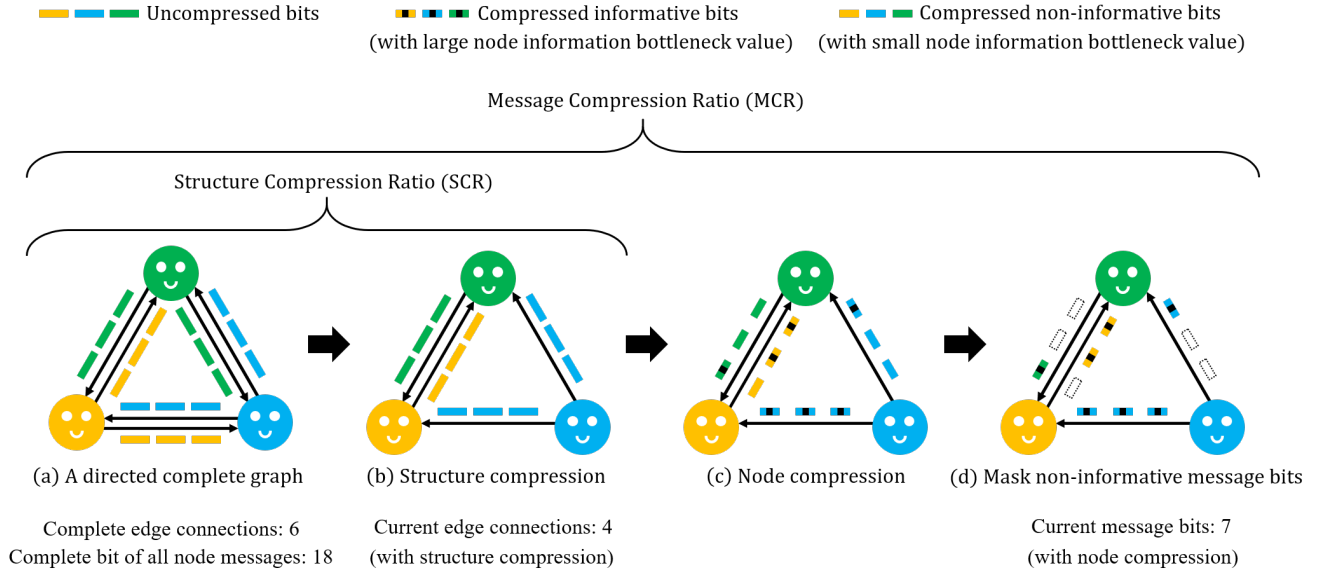


Figure 8: Schematic diagram of calculation of SCR and MCR in CGIBNet

Specifically, as is shown in Figure 8(b), there are 4 edge connections in the communication graph after structure compression, then we have

$$\text{SCR} = \frac{N_{e,complete} - N_{e,compressed}}{N_{e,compressed}} \times 100\% = \frac{6 - 4}{6} = 33.33\%.$$

Message Compression Ratio (MCR). Recall the definition of MCR mentioned in Section 5.1. Let $N_{m,complete}$ denotes the message bits without compression and $N_{m,compressed}$ denotes the unmasked message bits with compression. Then, MCR is calculated as $N_{m,complete} - N_{m,compressed} / N_{m,complete} \times 100\%$.

Specifically, as is shown in Figure 8(c), the information of each bit is compressed after node compression learning and we can judge the importance of these bits based on their node information bottleneck as mentioned in Section 4.2. Figure 8(d) indicates that when the communication bandwidth is constrained, the non-informative bits are masked first. In this case, MCR is calculated as

$$\text{MCR} = \frac{N_{m,complete} - N_{m,compressed}}{N_{m,compressed}} \times 100\% = \frac{18 - 7}{18} = 61.11\%.$$

Since the mask of each bit is implemented as a binary number, it only consumes a negligible log-scale space compared to the length of the message. Also, we adopt diagonal covariance for message embedding in CGIBNet, thus the bits of the node message are uncorrelated and can be masked independently.

7.5 E. Environment

7.5.1 E.1 Traffic Control.

We take the easy map as an example to detail the implementation of the Traffic Control environment and the mechanism can be extended to medium and hard maps.

Initialization position. As is shown in Figure 9(a), each car will be randomly initialized in the colored grid (*i.e.*, straight road), so that they have more opportunities to emerge cooperative behavior in the intersection area.

Initialization route. As is shown in Figure 9(b), each car will randomly select one of the two possible routes. one is going straight (*i.e.*, solid line) and is denoted as route 1, the other is turning left (*i.e.*, dotted line) and is denoted as route 2.

Location coordinates. As is shown in Figure 9(c), we respectively display the horizontal and vertical coordinates on the map. Therefore, the coordinates of the car can be expressed as $(4, 5)$.

Local observation. The local observation o of each car is composed of its location and assigned route id. In order to facilitate network learning, we implement it as a one-hot vector. Specifically, since the location and route id of the car in Figure 9(c) are $(4, 5)$ and route 2

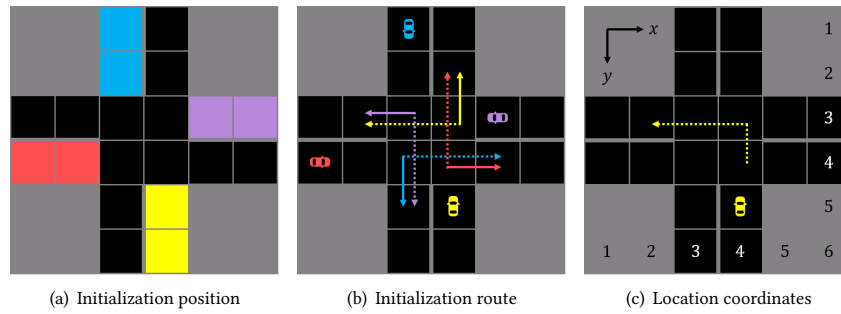


Figure 9: Experimental details of the easy map in the Traffic Control

respectively, the local observation o can be denoted as

$$o = (\underbrace{0, 0, 0, 1, 0, 0}_{x\text{-axis coordinate}}, \underbrace{0, 0, 0, 0, 1, 0}_{y\text{-axis coordinate}}, \underbrace{0, 1}_{route\ id}).$$

Global state. The global state is a simple concatenation of all local observations.

7.5.2 E.2 StarCraftII.



Figure 10: Snapshots of the StarCraftII scenarios

StarCraftII micromanagement aims to accurately control the individual units and complete cooperation tasks. In this environment, each enemy unit is controlled by the built-in AI (difficulty level) while each allied unit is controlled by a learned policy. The local observation of each agent contains the following attributes for both allied and enemy units within the sight range: distance, relative_x, relative_y, health, shield, and unit_type. In order to highlight the necessity of communication, we reduce the sight range of each agent from 9 to 2. The action space of each agent includes: noop, move[direction], attack[enemyid], and stop. Under the control of these actions, each agent can move and attack in various maps. The reward setting uses the default reward function, which is based on the hit-point damage dealt on the enemy units, together with special bonuses for killing the enemy units and winning the battle.

3b_vs_1h1m. As is shown in Figure 10(a), the positions of the 3 Banelings are randomly initialized on the map and they need to kill a Hydralisk that is assisted by a Medivac. 3 Banelings together can just blow up the Hydralisk. Thus they should take action in sync and attack the Hydralisk at the same time, otherwise Medivac will have extra time to heal the Hydralisk, leading to game defeat.

1o2r_vs_4r. As is shown in Figure 10(b), 1 Overseer has observed 4 enemy Reapers. Allied units of the Observer, 2 Roaches, need to find the Reapers and kill them. Since 1 Overseer and 4 enemy Reapers are initialized at the same location on the map while 2 Roaches are initialized to another location, the Overseer needs to continuously provide the enemy’s vision to help 2 allied Roaches find enemy units.

5z_vs_1ul. As is shown in Figure 10(c), 5 Zealots need to work closely to kill a powerful Ultralisk. Since the sight range of Zealots is severely limited, the communication mechanism can help them to emerge complex cooperation micro-skills.

1o10b_vs_1r. As is shown in Figure 10(d), this map is full of terrain obstacles, 1 Observer discovers 1 Roach, and its allies, 10 Banelings need to kill this Roach. Similar to the 1o2r_vs_4r map, since the initial positions of Overseer and Roach are inconsistent with that of Banelings, the Overseer needs to encode the Roach’s location information and send it to the allied Banelings to win the game.